Catal Lett (2009) 130:9–18
DOI 10.1007/s10562-009-9900-7

Catalytic Deoxygenation of Methyl-Octanoate and Methyl-Stearate on Pt/Al_2O_3

Phuong T. Do · Martina Chiappero · Lance L. Lobban · Daniel E. Resasco

Received: 26 December 2008 / Accepted: 7 February 2009 / Published online: 24 February 2009

Abstract The deoxygenation of methyl octanoate and methyl stearate over alumina-supported Pt was studied in both the vapor phase in a flow reactor and in the liquid phase in a semibatch reactor. The conversion of both methyl esters resulted in hydrocarbons with one carbon less than the fatty acid of the corresponding ester as the dominant products. In the vapor phase, acid and other oxygenates were observed in low concentrations, but they were not detected when the reaction was conducted in the liquid phase. Under He, condensation products (from esterification and ketonization) were observed. By contrast, under H_2, mostly paraffins were obtained. These results show promise to directly produce standard diesel components from biodiesel.

Keywords Biofuels · Deoxygenation · Methyl-octanoate · Methyl-stearate · Pt/Al_2O_3 catalyst

1 Introduction

In recent years, considerable attention has turned to the use of renewable resources to supply liquid transportation fuels. For example, diesel fuel can be produced from vegetable oil, which consists primarily of triglyceride compounds. Typically, the triglycerides are converted via transesterification with methanol to fatty acid methyl esters (FAMEs) which are commonly referred to as biodiesel. It is known that biodiesel have high cloud point and pour point [1, 2] which can lead to clogging of fuel filters and supply lines at low temperatures. In addition, due to the presence of oxygen in the biodiesel molecules, the heat content becomes 9–13% lower than that of conventional diesel fuels on a mass basis [3]. Finally, the chemical activity of the FAMEs limits biodiesel storage time or necessitates additives. Catalytic deoxygenation is a method that solves some of these problems [4, 5].

Deoxygenation, particularly decarboxylation, is a standard organic synthesis method. The decarboxylation of carboxylic acids to the corresponding hydrocarbons in the gas phase over heterogenous metal catalysts has been known for many years [6]. Liquid-phase deoxygenation of vegetable oils over supported metals, acidic, and basic catalysts has been reported by several groups [7–11]. Other studies have focused on elucidating the mechanism of deoxygenation of small carboxylic acids. For example, TPD studies of preadsorbed carboxylic acid on metals indicate that the selectivity to decarboxylation or decarbonylation depends on the metal-oxygen bond strength, which explains some of the activity trends observed on different metals [12]. In related work [13–15], researchers have found that the best catalyst for hydrogenation of a carboxylic acid to aldehyde/alcohol was a combination of a partially reducible oxide such as SnO_2 or TiO_2 with a noble metal, such as Pt. Oxygen removal occurs on the reducible oxide via an oxygen vacancy mechanism, while the metal provides dissociated hydrogen to reduce the oxides [16]. Reduction of carboxylic acids to corresponding alcohols and aldehydes has been both theoretically and experimentally examined over Cu, Pd, and Re catalysts [17–20]. Theoretical studies [20] have shown that the metal catalyzed hydrogenation of acetic acid requires a balance between C–O-bond-breaking, which results in aldehyde/

P. T. Do · M. Chiappero · L. L. Lobban (✉) · D. E. Resasco (✉)
School of Chemical, Biological, and Materials Engineering, University of Oklahoma, Oklahoma City, OK, USA
e-mail: llobban@ou.edu

D. E. Resasco
e-mail: resasco@ou.edu

alcohol products, and β C–H-bond-rupturing, which leads to decarboxylation/decarbonylation products.

Although most of the hydrogenation work in the literature is associated with carboxylic acids, some dealt with alkyl esters. For example, some authors have explored the reduction of methyl benzoate on Y_2O_3 catalyst [19]. Moulijn et al. [20] observed direct C–O cleavage of 1-(4-isobutylphenyl) ethanol on Pd/SiO_2 and Pd black. Dehydration of alcohols to form alkenes on γ-alumina also is well documented in the literature [21, 22].

More closely related to the present study, Murzin et al. [7–11] has reported the conversion of ethyl stearate, stearic acid, and tristearine to diesel fuel-like hydrocarbons over a series of commercial and supported catalysts. Reactions were carried out in semi-batch mode at 573–633 K and 0.6– 4.0 MPa under the flow of H_2, He or mixtures. They found that all three compounds were almost exclusively decarboxylated to n-heptadecane, but the selectivity and reaction pathway depended on both pH and gas composition. Focusing on the most effective catalyst Pd/C, they found that stearic acid conversion proceeded via decarboxylation to n-heptadecane, but ethyl stearate conversion proceeded through various pathways. Conversion of ethyl stearate to n-heptadecane occurred via stearic acid as an intermediate in the absence of H_2, but directly to C_{17} hydrocarbons via decarbonylation/decarboxylation in the presence of H_2.

These previous studies suggest that FAMEs (biodiesel) can be selectively deoxygenated for improved diesel fuel properties, but better control of selectivity and activity is necessary. In this work, we present results of deoxygenation of methyl stearate ($CH_3(CH_2)_{16}COOCH_3$, a representative biodiesel molecule) and methyl octanoate ($CH_3(CH_2)_7COOCH_3$, a model molecule) over alumina-supported Pt catalyst. Methyl octanoate was chosen as a model compound for ease of product identification in order to facilitate identification of reaction pathways. Methyl stearate was selected as representative of typical biodiesel FAMEs. In these studies, gas mixture and reaction temperature were varied. Gas- and liquid-phase analyses were performed in both reactions in both hydrogen and helium atmospheres in order to understand the impact of gaseous hydrogen on different reaction pathways, and to better identify the pathways that result in desired products as well as undesired coke precursors. Kinetic parameters for methyl stearate deoxygenation on Pt were estimated using a general power law rate expression.

2 Experimental

2.1 Catalyst Preparation

γ-alumina (HP-140 from Sasol) and titania (P-25 from Degussa) were used as catalyst supports. Platinum was incorporated by incipient wetness impregnation using aqueous solutions of chloroplatinic acid hexahydrate (Aldrich) to obtain a 1 wt% Pt loading. After impregnation the samples were kept at ambient temperature for 4 h, then dried at 383 K overnight, and finally calcined in flowing air (100 mL/min) at 673 K for 2 h.

2.2 Catalyst Characterization Techniques

The catalysts were characterized by using temperature-programmed reduction (TPR), CO chemisorption, and X-ray photoelectron spectra (XPS). TPR experiments were carried in a gas mixture of 5% H_2 in Ar (25 cm^3/min) over 75 mg of catalyst samples. The temperature was linearly increased to 973 K at 10 K/min. The effluent gases were analyzed using online SRI 110 thermal conductivity detector (TCD). Dynamic CO chemisorption was measured on 50 mg of catalyst sample, reduced in H_2 flow (100 cm^3/min) at 603 K (10 K/min ramp) for 1.5 h before switching to He (100 cm^3/min) at 603 K for 0.5 h to remove surface-adsorbed H. Then, 100μL pulses of CO were sent over the sample at 298 K. After the surface became saturated with CO, as indicated by the online detector, the ratio of CO uptake to the metal content (CO/Pt) was calculated. XPS spectra were obtained on a Physical Electronics PHI 5800 ESCA system equipped with an Al$K\alpha$ X-ray anode operated at 350 W and 15 kV. The base pressure of the UHV XPS chamber was $\sim 1.0 \times 10^{-8}$ Torr. A 400 μm spot size and 187.85 eV pass energy were implemented during the data acquisition. For XPS analysis of the reduced samples, two catalysts were pre-reduced in flow of H_2 (100 cm^3/min) at 603 K, and then transferred to an ex situ cell in a He glove bag to avoid exposure to air.

2.3 Catalytic Activity Measurements

2.3.1 Gas-Phase Conversion of Methyl Octanoate

The reactions of methyl octanoate ($CH_3(CH_2)_7COOCH_3$, MeOct, Acros) were carried out in a fixed-bed tubular reactor (1/2" OD stainless steel tube), equipped with a thermo well in the center of the catalyst bed. The catalyst was diluted with an inert material (α-alumina from Aldrich) to mitigate reaction heat effects. Catalyst particle diameter was less than 200μ to avoid mass transfer issues. Reactions were conducted in the gas phase at 603 K, at atmospheric pressure and using a H_2/hydrocarbon feed molar ratio of 40. The catalyst was first reduced for 1.5 h under flowing H_2 at 603 K. After reduction, the liquid reactant was fed using an Isco LC-500 high-pressure syringe pump. The line after the reactor was heated up to 543 K to maintain products and reactant in the gas phase. Reactor effluent was analyzed online using a Hewlett Packard 6890 GC. Product

identifications were using a Shimadzu GC-MS-P500. Chemical standards were also used to confirm product identification.

2.3.2 *Liquid-Phase Conversion of Methyl Stearate*

The conversion of methyl stearate ($CH_3(CH_2)_{16}COOCH_3$) was conducted at different temperatures (623, 610, 598 and 573 K) and 0.69 MPa in a 300 mL stirred reactor (Parr Corporation). After placing 1.0 g of 1% Pt/Al_2O_3 catalyst in the reactor, He was passed through to displace any air left in the vessel. Next, the catalyst was reduced for 2 h at 473 K under a constant flow of H_2. The reactor was then heated to the desired operating temperature, after stabilization the liquid feed was injected into the reactor. The feed was prepared by dissolving 4.7 g of methyl stearate in 134 mL of tetradecane solvent. The reaction was conducted in semi-batch mode, in which either H_2 or He gas was continuously passed through the reactor to remove the light gases (CO_2, CO and CH_4) produced by the reaction. Mechanical stirring at 500 rpm kept the catalyst suspended and prevented external mass transfer limitations. The typical reaction time (from the moment the reactor temperature returned to the desired value following feed injection) was 5 h. Liquid (reactor contents) and gas (reactor effluent) samples were taken every hour and were analyzed by gas chromatography. Liquid samples, diluted in heptane, were analyzed using a SRI 8610C Gas Chromatograph equipped with a nonpolar capillary column and a flame ionization detector. Several chemical standards such as heptadecane, octadecane and stearic acid were used to identify products. Gas samples were analyzed in a CARLE Series 400 Analytical Gas Chromatograph equipped with a Thermal Conductivity Detector.

3 Results and Discussions

3.1 Catalyst Characterization Analysis

Figure 1 shows the temperature-programmed reduction of Pt/Al_2O_3 and Pt/TiO_2 catalysts. For the alumina-supported catalyst, two reduction peaks are evident in good agreement with other TPR reported in the literature [23]. The hydrogen consumption peak at low temperature is due to reduction of Pt oxide particles that do not interact strongly with the alumina, while the high-temperature peak is associated those strongly interacting with it [24]. Decomposition of the Pt precursor that remains after the calcination step may also shift the reduction temperature. The reduction temperature chosen for the reaction (603 K) is a compromise between maximum reduction and minimum particle growth by high-temperature sintering. It must

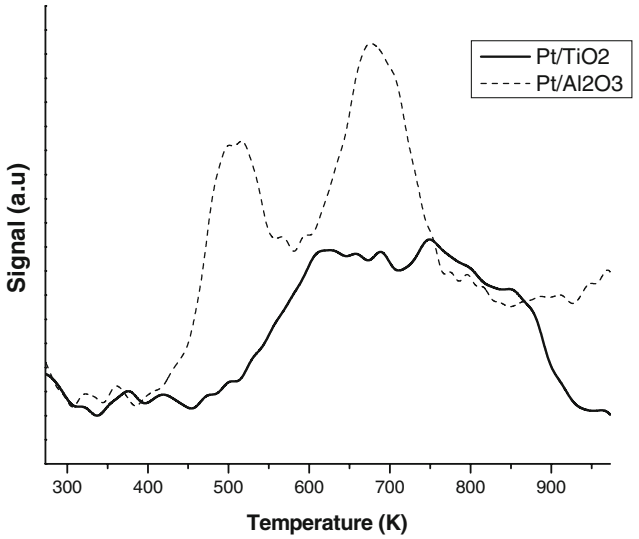

Fig. 1 Temperature-programmed reduction (TPR) of 1 wt% Pt/Al_2O_3 (*dashed line*) and 1 wt% Pt/TiO_2 catalysts (*solid line*)

be taken into consideration that during the pre-reduction step, a much higher hydrogen pressure than in the TPR experiments is employed, which will enhance the reduction of Pt oxides. Therefore, while a small fraction of PtO_x species stabilized by alumina support might not be reduced, a high CO/M ratio of Pt/Al_2O_3 catalyst (shown in Table 1) was still obtained. On the titania-supported catalyst, reduction of PtO_x stabilized by TiO_2 plus partial reduction of some TiO_2 support species lead the board peak in TPR profile of Pt/TiO_2 catalyst [24]. Since reduction of Pt/TiO_2 performed at high temperature might result in strong metal-support interaction, which leads to loss of Pt active sites [25], this catalyst has also been chosen to reduce at 603 K.

The XPS results for the oxidized and reduced catalysts are shown in Table 2. The pre-reduced sample of Pt/Al_2O_3 shows a high fraction of metallic Pt after 603 K reduction, which together with the TPR and CO-chemisorption data described above indicate that 603 K is a suitable reduction temperature. For the titania-supported catalyst, Pt appears only partially reduced after 603 K reduction. It must be taken into account that the residual Cl from Pt precursor (chloroplatinic acid hexahydrate) in both reduced samples probably generates some residual acidity, which is likely to participate in side reactions such as isomerization, cracking and transeterification during methyl octanoate reactions.

Table 1 Physical characteristics of the catalysts investigated

Catalysts	Pt wt%	Support surface area (m^2/g)	CO/Pt
Pt/Al_2O_3	1.0	220	0.9
Pt/TiO_2	1.0	50	–

Table 2 X-ray photoelectron spectra (XPS) data of 1 wt% Pt/Al_2O_3 and 1 wt% Pt/TiO_2 catalysts

Sample	Atomic surface concentration (%)					Atomic ratios		
	O (1s) (%)	Al (2p) (%)	Ti (3d) (%)	Cl (2p) (%)	Pt (4d) (%)	Pt/Al	Pt/Ti	Cl/Pt
1 wt% Pt/Al_2O_3 (oxidized)	66.6	31.6	0.0	1.0	0.9	0.03		1.1
1 wt% Pt/Al_2O_3 (pre-reduced)	68.2	30.5	0.0	0.8	0.6	0.02		1.3
1 wt% Pt/TiO_2 (oxidized)	65.7	0.0	30.7	2.0	1.7		0.05	1.2
1 wt% Pt/TiO_2 (pre-reduced)	68.4	0.0	30.8	0.2	0.6		0.02	0.3

The pre-reduced samples are reduced ex situ in hydrogen at 603 K for 2 h and then transferred into XPS without exposure to air

3.2 Gas Phase Conversion

3.2.1 Formation of C_7 and C_8 Hydrocarbons

The conversion of methyl octanoate over Pt/γ-Al_2O_3 catalyst in the vapor phase yields various products including hydrocarbons (C_7 and C_8 alkane and alkenes), other oxygenates (octanal, 1-octanol, octanoic acid), condensation products (diheptyl ketone, n-pentadecane and octyloctanoate), and light gases (CO, CO_2, CH_4, CH_3OH, and H_2CO). From the diesel fuel standpoint, the desirable products would be the straight chain hydrocarbons. In the studies reported here, at a high H_2/HC ratio, saturated C_7 and C_8 hydrocarbons are the dominant hydrocarbon products. Only a small fraction of unsaturated hydrocarbons and trace amounts of aromatics were obtained.

Table 3 shows the distribution of products from conversion of methyl octanoate at a time-on-stream of 1.0 h, excluding light gases, over a 1% Pt/γ-Al_2O_3 catalyst under flow of hydrogen at various W/F. Almost no cracking products are observed for conversions up to 60%. At higher conversions, small fractions of light hydrocarbons are detected. C_7 hydrocarbons are the major product, while C_8 hydrocarbons and other oxygenates account for less than 10% of the products. From Table 3, at low conversion (below 5%), the calculated selectivity to the C_8 hydrocarbon is negligible, while the combined octanal—octanol selectivity is around 10% and that to octanoic acid is close to 40%. At higher conversions, selectivity of octanal and 1-octanol drops with increasing selectivity of C_8 hydrocarbons.

Both C_7 and C_8 hydrocarbons are the target deoxygenation products of methyl octanoate conversion, so it is valuable to understand the reaction pathways that result in the formation of these two hydrocarbon products, as well as the pathways leading to undesirable condensation (heavy) products, which not only reduce selectivity but can also deactivate the catalyst. The appearance of mostly C_7 hydrocarbons and octanoic acid at low conversions suggests that C_7s can be produced by two parallel paths via decarboxylation and decarbonylation. That is, indirectly via octanoic acid or directly from methyl octanoate. The metal-catalyzed decarbonylation of one-oxygen-containing compounds such as aldehydes, alcohols and ketones to the corresponding hydrocarbons with one C less than the parent oxygenated feed is a well-known reaction [26, 27]. Similar results were found by Murzin in the conversion of ethyl stearate (C_{18}) over Pd/C catalysts in presence of H_2, yielding mostly n-heptadecane [7]. As illustrated in the reaction scheme shown in Fig. 2, 1-octanol, octanal via hydrogenation/hydrogenolysis, while heavier oxygenates can be obtained by condensation reactions such as ketonization and transesterification. These oxygenates can also contribute to the production of C_7 hydrocarbons via decarboxylation/decarbonylation. In contrast, C_8 hydrocarbons are not primary products, i.e., they are formed via a 2-step reaction. As depicted in Fig. 2, C_8 hydrocarbons, which are the hydrogenated products in this case, are

Table 3 Product distribution from reaction of methyl octanoate over 1 wt% Pt/Al_2O_3 catalyst at TOS of 1 h and in the flow of H_2 ($p = 101$ kPa, $T = 603$ K, H_2/Oxygenate = 30)

W/F (h)	0.01	0.02	0.03	0.10	0.17	0.34	0.60	0.86	1.20
Conversion	1.5%	8.3%	16.9%	19.8%	28.2%	57.1%	61.4%	85.7%	97.8%
	Yield (%)								
Cracking compounds	0.0	0.0	0.0	0.0	0.0	0.0	0.2	1.2	2.9
Total C_7 hydrocarbons	0.6	6.5	14.6	15.2	23.5	46.4	53.1	75.0	89.5
Total C_8 hydrocarbons	0.0	0.1	0.2	0.3	0.2	0.9	1.8	2.4	5.0
1-Octanol + octanal	0.2	0.3	0.4	0.4	0.5	0.8	0.3	0.3	0.2
Octanoic acid	0.6	0.7	1.1	2.5	1.5	6.2	4.5	4.7	0.1
Heavy products	0.2	0.7	0.6	1.4	2.4	2.8	1.5	2.0	0.0

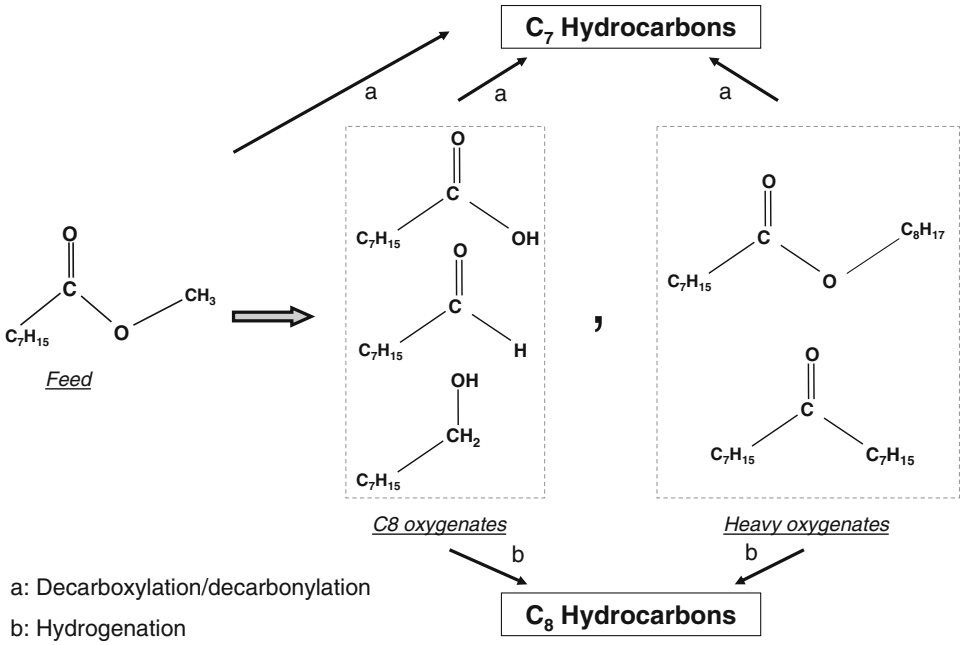

Fig. 2 Formation of C_7 and C_8 hydrocarbons from methyl octanoate

directly derived from C_8 aldehyde/alcohol, which originally are generated from either the methyl ester or the acid.

In a separate experiment, when we fed 1-octanal over 1% Pt/γ-Al_2O_3, we observed C_7 hydrocarbons as the main product, with much less C_8 hydrocarbons and 1-octanol. This result supports the concept that in the methyl octanoate conversion, primary products are octanoic acid and C_8 aldehyde/alcohol, which subsequently mainly convert to C_7 hydrocarbons via decarbonylation and to a lesser extent to C_8 hydrocarbons via C–O hydrogenolysis. No C_6 or lower hydrocarbons (from demethylation of C_7) have been observed, which suggests that the alumina-supported Pt catalyst has negligible cracking activity.

In summary, these studies suggest that in the presence of hydrogen conversion of methyl octanoate to octanoic acid is dominant (Table 3). Formation of C_7 hydrocarbons can stem from direct decarboxylation/decarbonylation of the ester, acid, aldehyde, and alcohol. At the same time, C_8 hydrocarbons come from direct C–O hydrogenolysis of the alcohol/aldehyde following hydrogenation of the ester and acid.

3.2.2 *Formation of Heavy Products*

To maximize the conversion of the methyl esters to fuel-like products (C_7 and C_8 hydrocarbons), it is necessary to minimize the production of heavy condensation compounds such as diheptyl ketone, n-pentadecane and octyloctanoate. According to Ponec et al. [28], the symmetrical ketone is formed via the interaction of two adjacent carboxylate species on the oxide surface. A second observed heavy product in our experiments was octyloctanoate, which results from either esterification of octanoic acid with 1-octanol or transesterification of methyloctanoate with the alcohol. These two reactions can be catalyzed by Brönsted acid sites [29]. A third heavy product, n-pentadecane, is probably formed via C–O hydrogenolysis of the diheptyl ketone. Even though the yields of all three products are quite low in the presence of hydrogen, information on how these products form will assist to reduce the formation of those undesirable products. The ketonization reaction is only favored under a hydrogen-deficient environment. Therefore, when the oxides were reduced by the presence of spilled-over hydrogen from Pt (on Pt/TiO_2 catalyst), the ketone formation on TiO_2 was greatly suppressed by the availability of hydrogen on reduced TiO_2 surface. Since none of the hydrogenated product of the ketone, a secondary alcohol, was detected, the heavy hydrocarbon is probably produced via C–O hydrogenolysis. Barteau et al. [30] also observed propane, the product from acetone, over Pd/CeO_2 and Co/CeO_2 catalysts. Although the presence of surface Cl, which may generate acid sites, is still detected on the reduced Pt/Al_2O_3 (as shown by XPS in Table 2) the production of octyloctanoate remains low throughout the course of the reaction. The yields of undesirable heavy ketone and hydrocarbon are also suppressed by the presence of hydrogen.

3.2.3 *Comparison Between Pt/Al_2O_3 and Pt/TiO_2 Catalysts*

One of the characteristics of decarboxylation and decarbonylation is the loss of carbon via release of CO_2 and CO, respectively, which results in product with one C less than the feed. By contrast, catalysts that are active for C–O

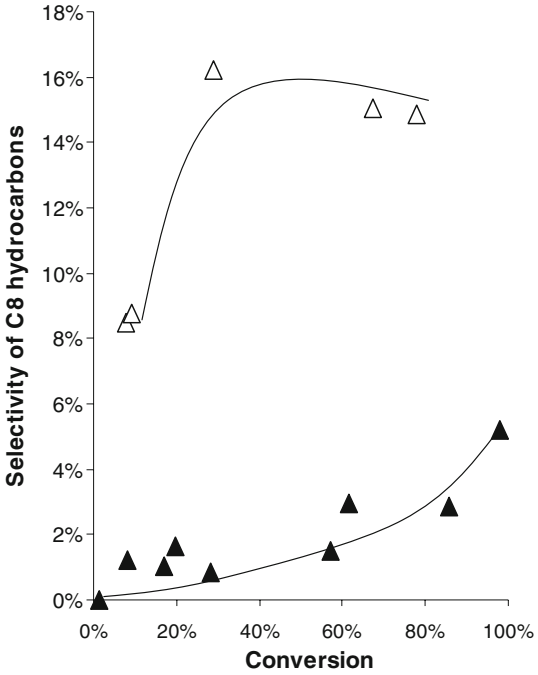

Fig. 3 Selectivity of C_8 hydrocarbons as varying methyl octanoate conversion for 1 wt% Pt/Al_2O_3 (*filled*) and 1 wt% Pt/TiO_2 (*unfilled*)

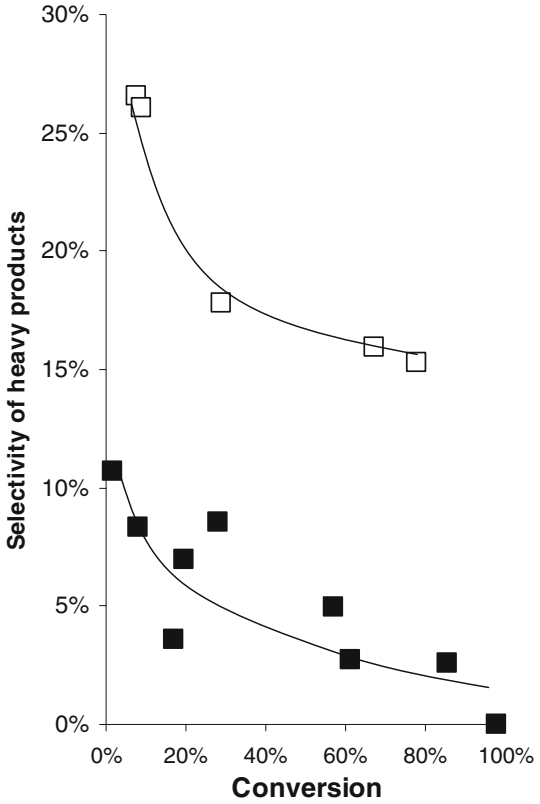

Fig. 4 Selectivity of heavy products as varying methyl octanoate conversion for 1 wt% Pt/Al_2O_3 (*filled*) and 1 wt% Pt/TiO_2 (*unfilled*)

hydrogenolysis may reduce the carbon loss. In this case, we compare the conversion of methyl octanoate to C_8 hydrocarbons as opposed to C_7 hydrocarbons. In this sense, Pt/TiO_2 catalyst seems to be a better candidate since selectivity to C_8 hydrocarbons is significantly higher for Pt/TiO_2 than for Pt/Al_2O_3 as illustrated in Fig. 3. This difference is due to a higher C–O cleavage activity, perhaps related to the higher reducibility of the titania support compared to alumina. It is well known that spilled-over hydrogen from Pt to titania helps reducing TiO_2 into TiO_x ($x < 2$) at 603 K [25, 31]. The large availability of Ti cations can enhanced the adsorption of methyl octanoate via bond of an ester oxygen and a Ti cation. The activation of the C–O bond can occur through the so-called oxygen-vacancy mechanism [32]. Titania may appear attractive for enhancing the C–O cleavage reaction. However, a drawback of titania-supported Pt catalyst is its high selectivity towards production of heavy products (i.e. symmetrical ketone and octyloctanoate) as shown in Fig. 4. Given the chlorine content of pre-reduced TiO_2 and Al_2O_3 from the XPS data in Table 2, one could predict that the density of acid sites for transesterification reaction of methyl octanoate would be higher on Al_2O_3 than on TiO_2. Higher acidity would lead to higher production of octyloctanoate from alumina catalyst. However, the contribution of the formation of symmetrical ketone via oxygen vacancy sites dominates, as seen in the heavy product distribution. Although the spilled-over hydrogen from Pt helps limiting ketone formation, methyl octanoate molecules adsorb preferably on reduced TiO_2 surface than on the more refractory Al_2O_3 surface. Exposed Ti cations can interact with two acid molecules (or methyl esters) to form one symmetrical ketone molecule.

3.2.4 Deactivation Study

Figure 5 displays the conversion of methyl octanoate over the Pt/Al_2O_3 catalyst as a function of time on stream, at a W/F of 0.6 h. It is seen that, in H_2 flow, the conversion drops from 61% to 42% over 5-h on stream. The observed deactivation is due to site blocking by oligomerization of unsaturated hydrocarbons and heavy compounds (i.e. symmetrical ketone) that lead to coke. This deactivation is accelerated when no H_2 is used. The first conversion point under He gas is 40% compared to 61% for hydrogen. Moreover, at a TOS of 2 h, the conversion further drops to 15%. This dramatic drop in catalyst activity parallels the increase in unsaturated hydrocarbons and heavy substances observed in the product distribution. Instead of the C_7 and C_8 alkanes that dominate in the presence of excess H_2, alkenes become dominant in He. Interestingly, a large activity recovery is observed when the carrier gas is switched from He to H_2. At the same time, saturated hydrocarbons are again the dominant products and formation of heavy products is much inhibited.

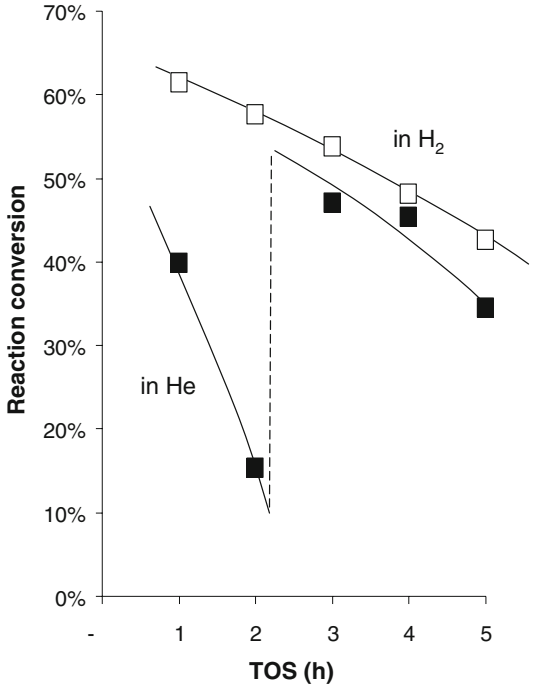

Fig. 5 Conversion of methyl octanoate over 1 wt% Pt/Al_2O_3 catalyst as a function of time on stream; $p = 101$ kPa, $T = 603$ K, H_2/feed ratio = 30, $W/F = 0.6$ h. *Open symbols*: reaction in flow of H_2. *Full symbols*: reaction in flow of He for first 2 h, then in flow of H_2

3.3 Liquid Phase Conversion

Since the reactions were performed in liquid phase, it is important to check whether mass transfer limitations are present and may be masking some of the kinetic measurements. Therefore, standard calculations of mass transfer rates were done using empirical equations. Diffusion coefficients were calculated using the Stokes-Einstein equation which can be applicable for large molecules like those used in this study. From this, the external mass transfer coefficients (k_c) were obtained. By including the appropriate catalyst information we obtained a maximum methyl stearate mass flux value of $N_{MS} = 6.70 \times 10^{-2}$ g/s), which is two orders of magnitude greater than the observed reaction rate.

At the same time, the Weisz-Prater Criterion was used to evaluate the possibility of internal diffusion effects. The N(W-P) = {observed rate. (particle radius)^2/(C_s D_{eff})} was found to be much less than 0.3, which indicates that with the small pellet size used in this study (less than 0.18 mm) there are no internal diffusion limitations.

The molar fraction of hydrogen solubilized in the feed for the runs conducted under hydrogen was estimated to be 0.018 [33]. When comparing with molar fraction of the feed in liquid phase, it could be concluded that the reactions were performed under excess of hydrogen.

In order to compare the liquid phase reaction was the gas phase reactions shown above, methyl octanoate was fed in the liquid phase. The reaction of methyl octanoate in liquid phase over 1% Pt/Al_2O_3 catalyst resulted in majority of C_7 hydrocarbons in the liquid phase and mostly CO in the gas phase. That is, both in the gas phase and in the liquid phase reactions, decarbonylation is the major reaction pathway. However, in most of the liquid-phase runs reported in this study, methyl stearate was used, to represent a molecule that is more common from natural oil transesterification processes. The primary products in the conversion of methyl stearate were heptadecane, 1-heptadecene, octadecane and heavy products in the liquid phase; CO_2, CO and CH_4 in the gas phase. Comparison of the yield of the different liquid products under flow of two different gases, H_2 and He, versus time can be seen in Figs. 6 and 7. After 5 h, the conversion of methyl stearate at 598 K and 690 kPa under H_2 flow was approximately 64% (Fig. 6). The final conversion after 5 h at the same temperature but under He flow was 42% (Fig. 7). The lower conversion under He is probably due to a faster catalyst deactivation, as it was observed in the gas phase when switching from H_2 to He (Fig. 5). In both cases, C_{17} paraffins were the major compounds formed, but under He, C_{17} and C_{18} alkenes were also observed, whereas under H_2, no alkenes were detected. The alkenes probably lead to coke precursors, deactivating the catalyst. Heavy products such as ketones were seen in both cases. These compounds would also be expected to contribute to catalyst deactivation.

Analogous to the case of methyl octanoate, we observed with methyl stearate high yield and high selectivity (>90%

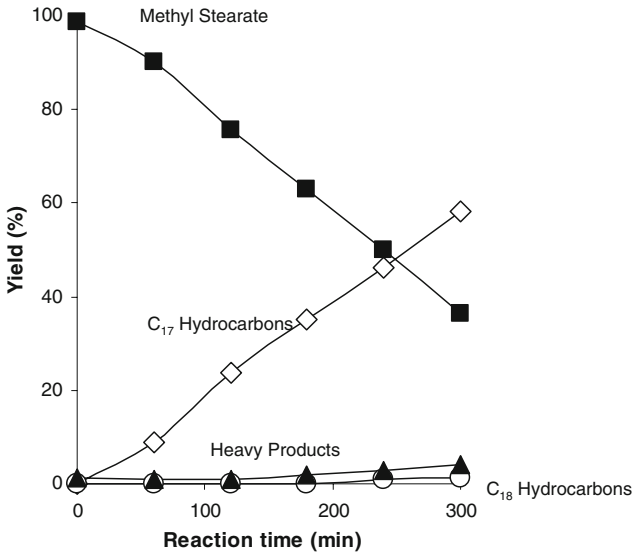

Fig. 6 Product distribution from methyl stearate reaction over 1 wt% Pt/Al_2O_3 catalyst in flow of H_2; $p = 690$ kPa, $T = 598$ K

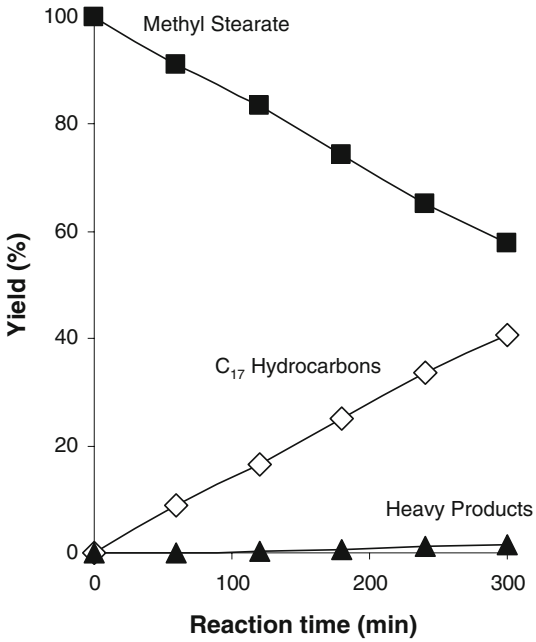

Fig. 7 Product distribution from methyl stearate reaction over 1 wt% Pt/Al_2O_3 catalyst in the flow of He ($p = 690$ kPa, $T = 598$ K)

after 5 h) towards C_{17} hydrocarbons, with essentially no cracking. Moreover, no C_{16} hydrocarbons were found which confirms that demethylation does not significantly occur. Some traces of C_{18} were found, especially under H_2 flow (Fig. 6), suggesting that this compound comes from deoxygenation of aldehyde and/or alcohol intermediates. These intermediates were not seen in the liquid samples, possibly because they remain adsorbed on the catalyst and/or they are highly reactive. As discussed previously, the C_{18} compound could be formed on metal sites via C–O hydrogenolysis on Pt sites [18] or on oxygen vacancies as suggested by Ponec et al. [16].

Condensation products were seen in both cases (Figs. 6, 7). Based on the boiling point of these species, these heavy products are most likely ketonization and transterification products, i.e., C_{35} specie formed from two carboxylates. Ponec et al. [28] have pointed out that ketonization reaction is catalyzed by oxides. When we contacted methyl stearate with the bare Al_2O_3 support under the same reaction conditions, production of heavy symmetrical ketone and ester was significant whereas C_{17} hydrocarbon selectivity was low (Table 4). Based on findings from the methyl octanoate study, not only ketonization but also esterification/transterification reactions may result in condensation products.

Figure 8 shows the evolution of gas-phase products with reaction time on $1\%Pt/Al_2O_3$ at 598 K and 690 kPa under H_2 and He flow in the liquid phase. In both cases, CO was the main product. Minor amounts of CO_2 were observed

Table 4 Product distribution of methyl stearate over Al_2O_3 catalyst in the flow of H_2 after 5 h reaction

Products	$p = 690$ kPa, $T = 562$ K		$p = 690$ kPa, $T = 611$ K	
	Yield (%)	Selectivity (%)	Yield (%)	Selectivity (%)
C_{17} Hydrocarbons	0.8	8.6	0.6	2.6
Diheptadecyl ketone	1.5	15.4	6.8	28.6
Octadecyl stearate	7.4	76.1	16.4	68.9

Two columns on the left: $p = 690$ kPa, $T = 562$ K. Two columns on the right: $p = 690$ kPa, $T = 611$ K

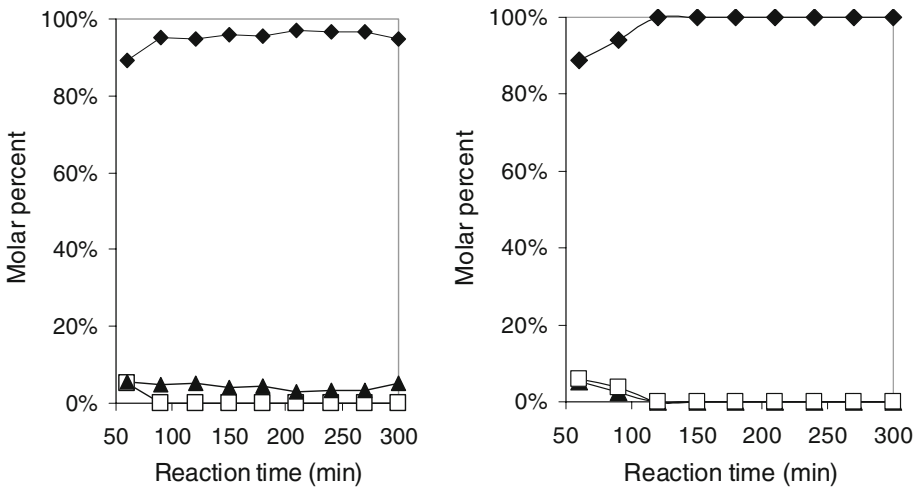

Fig. 8 Composition of the gas phase products (excluding the carrier) from methyl stearate reaction over 1 wt% Pt/Al_2O_3. Reaction was conducted at 598 K and 690 kPa under flow of H_2 (*left*) or He (right). CO (diamonds), CH_4 (*squares*), CO_2 (*triangles*)

while CH_4 was only detected at the beginning of the reaction. These results suggest that methyl stearate decarbonylates directly to form CO. The fact that methanol is not observed may be explained by further reaction to CO and H_2.

The rate of conversion of methyl stearate in the semi-batch reactor was fitted to a general rate law expression as follows:

$$\text{Rate} = -\frac{dC_{ms}}{dt} = k\, e^{-E/RT} C_{ms}^{n} \quad (1)$$

where, k is the rate constant, C_{ms} the concentration of methyl stearate, and n the reaction order.

The experimental data at different temperatures were fitted simultaneously, using common kinetic parameters. The fits are shown in Fig. 9. The parameters resulting from the fit are shown in Table 5. The activation energy, based on this rate expression, was 106.53 kJ/mol, significantly higher than the apparent activation energy value of approximately 58.60 kJ/mol found by Murzin et al. [11] in the conversion of ethyl stearate over a 5%Pd/C catalyst. The order of the reaction obtained in the fitting is near 1/3, which indicates that adsorption competition plays an important part in the reaction.

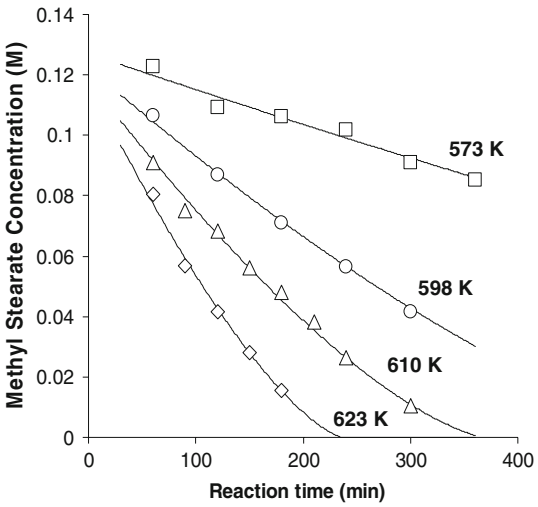

Fig. 9 Experimental data and fitting for methyl stearate conversion at different reaction temperatures. Reactions were operated 690 kPa under the flow of H_2

Table 5 Fitted kinetic parameters for Eq. 1

Parameters	Value	Unit
k_o	2.08E + 04	1/s
E	106.53	kJ/mol
n	0.31	

4 Conclusions

High activity and selectivity toward diesel-like hydrocarbons from both model compound and real vegetable oil feedstock (methyl octanoate and methyl stearate) can be successfully achieved with $1\%Pt/\gamma\text{-}Al_2O_3$. When feeding methyl octanoate, a mixture of C_7 alkane and alkenes, which results from decarbonylation or decarboxylation of the ester, acid and other 1-oxygen-containing compounds, are dominant products. C_8 hydrocarbons are also formed but in much smaller quantities. The C_8 compounds are originated from successive removal of oxygen via either oxygen vacancies created on the gamma-alumina support or direct C–O hydrogenolysis on the metal sites or a combination of dehydration and hydrogenation routes. Under similar conditions, 1% Pt/TiO_2 shows higher C_8 hydrocarbon selectivity than 1% Pt/Al_2O_3 due to a larger oxygen vacancy availability on the titania support. When the reaction is carried out under hydrogen atmosphere, formation of heavy products such as diheptyl ketone, n-pentadecane, and octyloctanoate are much suppressed compared to reaction carried out under inert gases.

The results from the liquid phase experiments show that the decarbonylation of methyl stearate over a heterogeneous catalyst, $1\%Pt/Al_2O_3$, produces heptadecane with high selectivity. The carrier gas used in the semibatch reactor plays an important role. Both the conversion and selectivity towards paraffin are higher under hydrogen than under an inert gas.

Acknowledgments This work has been funded by the Secretary of Energy of the State of Oklahoma and the Oklahoma Bioenergy Center. The XPS spectra were obtained by Dr. Min Shen.

References

1. Geyer SM, Jacobus MJ, Lestz SS (1984) Trans ASAE 27:375
2. Peterson CL, Korus RA, Mora PG, Madsen JP (1987) Trans ASAE 30:28
3. Demirbas A (2003) Ener Convers Manag 44:2093
4. Da Rocha Filho GN, Brodzki D, Djega-Mariadassou G (1993) Fuel 72:543
5. Gusmao J, Brodzki D, Djega-Mariadassou G, Frety R (1989) Catal Today 5:533
6. Maier WF, Roth W, Thies I, Schleyer PvR (1982) Chem Ber 115:808
7. Kubickova I, Snare M, Eranen K, Maki-Arvela P, Murzin DY (2005) Catal Today 106:197
8. Snare M, Kubickova I, Maeki-Arvela P, Eraenen K, Murzin DY (2006) Ind Eng Chem Res 45:5708
9. Maeki-Arvela P, Kubickova I, Snre M, Eraenen K, Murzin DY (2007) Energy Fuels 21:30
10. Snare M, Kubickova I, Maki-Arvela P, Eranen K, Murzin DY (2005) Chem Ind 115:415
11. Snare M, Kubickova I, Maeki-Arvela P, Eraenen K, Waerna J, Murzin DYu (2007) Chem Eng J 134:29
12. Houtman C, Barteau A (1991) Surf Sci 248:57

13. Pestman R, Koster RM, Pieterse JAZ, Ponec V (1997) J Catal 168:255
14. Rachmady W, Vannice MA (2000) J Catal 192:322
15. Pei ZF, Ponec V (1996) Appl Surf Sci 103:171
16. Sakata Y, Tol-Koutstaal CAV, Ponec V (1997) J Catal 169:13
17. Natal Santiago MA, Sanchez-Castillo MA, Cortright RD, Dumesic JA (2000) J Catal 193:16
18. Pallassana V, Neurock M (2002) J Catal 209:289
19. King ST, Strojny EJ (1982) J Catal 76:214
20. Thakar N, Polder NF, Djanashvili K, Bekkum HV, Kapteijn F, Moulijn JA (2007) J Catal 246:344
21. Knözinger H, Scheglila A (1997) J Catal 17:252
22. Morávek V (1992) J Catal 133:170
23. De Miguel SR, Román-Martınez MC, Cazorla-Amorós D, Jablonski EL, Scelza OA (2001) Catal Today 66:289
24. Huizinga T, Van Grondelle J, Prins R (1984) Appl Catal 10:199
25. Haller GL, Resasco DE (1989) Adv Catal 36:173
26. McCabe RW, DiMaggio CL, Madix RJ (1985) J Phys Chem 89:854
27. Davis JL, Barteau MA (1989) J Am Chem Soc 111:1782
28. Pestman R, Koster RM, Duijne AV, Pieterse JAZ, Ponec V (1997) J Catal 168:265
29. López DE, Suwannakarn K, Bruce DA, Goodwin JG Jr (2007) J Catal 247:43
30. Idriss H, Diagne C, Hindermann JP, Kiennemann A, Barteau MA (1995) J Catal 155:219
31. Huizinga T, Prins R (1981) J Phys Chem 85:2156
32. Barteau MA (1993) J Vac Sci Technol A 11:2162
33. Florusse LJ, Peters CJ (2003) AIChE J 49:3260